Coupling between lattice vibrations and magnetism in Ising-like systems

Carles Triguero, Marcel Porta, and Antoni Planes
Departament d'Estructura i Constituents de la Matèria, Universitat de Barcelona, Diagonal 647, 08028 Barcelona, Catalonia, Spain
(Received 6 May 2005; revised manuscript received 19 October 2005; published 1 February 2006)

In this paper the bond proportion model is introduced as a prototype of a system with coupled magnetic and vibrational degrees of freedom. This model is generalized within the framework of cluster expansions in order to achieve invariance of the potential energy to a rotation of the crystal. First, the original bond proportion model is solved in the mean-field approximation and by means of numerical simulations. It has been found that the temperature and the smoothness of the magnetic phase transition depend on the strength of the magnetoelastic coupling. For a large enough entropy difference between the magnetic phases the phase transition becomes first order. This is evidenced by means of the computation of the magnetization, the elastic constants, and the total entropy. The numerical simulation of the modified bond proportion model has revealed significant differences with respect to the bond proportion model in the heat capacity around the phase transition and, consequently, in the entropy difference between the magnetic phases. Small differences in the elastic constants are also detected.

DOI: 10.1103/PhysRevB.73.054401 PACS number(s): 75.10.Hk, 63.70.+h, 64.60.Cn, 62.20.Dc

I. INTRODUCTION

In any solid at finite temperature, atoms are not fixed at any given lattice position, but rather they oscillate around these positions. In spite of the fact that in typical situations the amplitudes of these lattice vibrations are small (compared with the averaged lattice parameter), they enable us to deal with the basic thermal properties of solids as shown in any textbook on solid-state physics or statistical mechanics.[1] Nevertheless, they are rarely taken into account when properties arising from other degrees of freedom such as configurational, magnetic, etc., are studied. There are, however, a number of works where the influence of vibrations on such properties have been considered. These studies are essentially aimed at two different problems. On the one hand, the study of the critical behavior of compressible Ising lattices has been considered.[2] In this case, positional variables are included in an Ising spin model and the lattice parameter is allowed to fluctuate. This yields an effective Hamiltonian with renormalized exchange coupling constants. Results indicate that the universality class of these models can be different from the corresponding Ising class[2,3] and even that the transition can become first order.[4] Indeed, these models are relevant for Monte Carlo simulation studies in the isothermal-isobaric ensemble.[5]

On the other hand, there has been some interest in the study of the influence of lattice vibrations on the phase stability of substitutional alloys.[6] This category of problems, which emphasizes more on the vibrational features of the studied system, has generated increasing interest since the early 1990s due to the possibility of measuring the vibrational contribution to the entropy change between ordered and disordered phases in alloys.[7–9] This has led to a considerable amount of literature, which, to a large extent, has been reviewed in Ref. 6.

In the present paper we mainly adopt the latter viewpoint. The influence of vibrational degrees of freedom on the phase stability of systems that can be described by means of a generic Ising model is studied. This includes, among others, magnetic systems and substitutional alloys. Therefore we expect that our results are of general interest and useful for a deeper understanding of phase stability in a wide class of systems.

In addition to the more usual weak-coupling limit for which the contribution of the vibrational entropy is small, we will also consider the strong-coupling limit with a dominant contribution of this term. This is an interesting situation, where, for instance, antiferromagnetism (ferromagnetism) can be stabilized due to lattice vibrations in systems with ferromagnetic (antiferromagnetic) coupling. This situation gives rise to the so-called vibrational entropy-driven transitions between ordered phases, for which the high-temperature phase is stabilized due to its larger vibrational entropy.[10]

Vibrational effects are introduced in the high-temperature harmonic approximation within the framework of the bond proportion model[11] (BPM). In this model antiparallel spins are assumed to have a different stiffness than parallel spins. At a phase transition, the proportion of each type of bonds changes and the average stiffness of the system is modified. Typically vibrational degrees of freedom are integrated in order to obtain an effective Ising model. In contrast, in the present work vibrational degrees of freedom are explicitly modeled. While being more computationally demanding, this approach is the natural way which enables the explicit calculation at finite temperature of the change of the vibrational properties between the phases occurring in the system, as reflected by the behavior of the elastic constants (in general, phonon dispersion curves). This is interesting since experimental evidence of such changes have been reported for order-disorder[12] and magnetic transitions.[13–15] These results provide a direct proof of the coupling between vibrational and magnetic or configurational degrees of freedom.

The simplicity of the BPM is very appealing, but unfortunately this model does not properly take into account the required invariance relations to be satisfied by the free energy. In particular, if bending forces are present, invariance to rotations is not conveniently established.[16] In general, vio-

lation of this invariance may give rise to unphysical behavior of the calculated thermodynamic quantities such as elastic constants, heat capacity, etc. Therefore in the present paper we propose a modification of the BPM in order to achieve rotation invariance of the free energy. Since the BPM has been widely used in the literature,[6] we solve this model first, and afterwards, we analyze the differences between the thermodynamic quantities obtained from this model and the modified bond proportion model (MBPM).

The paper is organized as follows. In the next section we introduce the BPM and the MBPM. The mean-field solution of both models for the ferromagnetic and antiferromagnetic cases is given in Sec. III. In the next section numerical simulations which combine a Monte Carlo method for the magnetic degrees of freedom and a Langevin technique for the vibrational degrees of freedom is presented in the ferromagnetic case. Comparison of simulation results for the nonrotational invariant model and for the generalized model is shown. Finally, in Sec. V we summarize and conclude.

II. MODELING

The BPM is described in detail in Ref. 6. In this section we develop this model within a more general framework: the spin cluster expansion of a force constants model. Within this framework it is straightforward to generalize the BPM by introducing additional terms in the expansion in such a way that all the required invariance relations are satisfied. This is done in Sec. II B.

A. Bond proportion model

In the present work the configurational degrees of freedom are localized spin-1/2 variables S_n that can take values $S_n = \pm 1$, so that the system under consideration is a magnetic solid. The vibrational variables are defined as the moments, $\mathbf{p}_n$, and displacements of the atoms from their associated lattice sites $\mathbf{u}_n$. The index n will label a given atom in the lattice. The model Hamiltonian is formulated for a simple (3d) cubic (SC) lattice as a sum of a magnetic (m) and a vibrational (v) term,

$$\mathcal{H} = \mathcal{H}_{\mathrm{m}} + \mathcal{H}_{\mathrm{v}}. \tag{1}$$

The magnetic term is a simple Ising model,

$$\mathcal{H}_{\mathrm{m}} = -\frac{1}{2}\sum_{nn'} J_{nn'} S_n S_{n'}, \tag{2}$$

where the summation extends over all the atoms. The vibrational term includes a kinetic energy term and a potential-energy term. The potential energy term is expanded up to second order about the lattice sites (not necessarily equilibrium sites). That is,

$$\mathcal{H}_{\mathrm{v}} = \sum_n \frac{p_n^2}{2m} + \sum_n \sum_i \frac{\partial V}{\partial u_n^i} u_n^i + \frac{1}{2}\sum_{nn'} \sum_{ii'} \frac{\partial^2 V}{\partial u_n^i \, \partial u_{n'}^{i'}} u_n^i u_{n'}^{i'}, \tag{3}$$

where the indices i, i' denote the components of the atomic displacement vectors. The coupling of the magnetic and vibrational degrees of freedom is introduced through a dependence of the potential-energy expansion coefficients on the magnetic spin variables. Notice that, in general, this coupling reduces the symmetry of the vibrational Hamiltonian since the symmetry of the spin configuration is lower than the symmetry of the underlying SC lattice. For the sake of simplicity, the linear coefficients of the potential-energy expansion are set to zero. This means that we neglect the atomic relaxations due to magnetic disorder. Taking into account cluster expansion theory,[17] the force constants are expressed as the following expansion in spin clusters:

$$\Phi_{nn'}^{ii'} \equiv \frac{\partial^2 V}{\partial u_n^i \, \partial u_{n'}^{i'}} = \sum_C (\xi_C)_{nn'}^{ii'} \prod_{n'' \in C} S_{n''}, \tag{4}$$

where the summation extends over all possible spin clusters in the lattice, and the product extends over all spins in a given cluster. Within the BPM approximation only the empty cluster and the pair cluster nn' will be considered in the computation of the force constant $\Phi_{nn'}^{ii'}$ with $n \neq n'$. That is,

$$\Phi_{nn'}^{ii'} \approx (\xi_0)_{nn'}^{ii'} + (\xi_{nn'})_{nn'}^{ii'} S_n S_{n'}, \quad n \neq n'. \tag{5}$$

The force constants involving a single site, $\Phi_{nn}^{ii'}$, can then be computed using the relation

$$\Phi_{nn}^{ii'} = -\sum_{n' \neq n} \Phi_{nn'}^{ii'}, \tag{6}$$

which is the condition of invariance of the potential energy with respect to a global translation of the crystal. In the BPM the coupling parameters $(\xi_{nn'})_{nn'}^{ii'}$ are taken to be[6]

$$(\xi_{nn'})_{nn'}^{ii'} = \lambda (\xi_0)_{nn'}^{ii'}, \tag{7}$$

where λ is a constant, and the coefficient of the empty cluster, $(\xi_0)_{nn'}^{ii'}$, is invariant under the symmetries of the crystal lattice. Thus the force constants are written as

$$\Phi_{nn'}^{ii'} = (\xi_0)_{nn'}^{ii'} (1 + \lambda S_n S_{n'}), \quad n \neq n'. \tag{8}$$

$\lambda = 0$ corresponds to the case in which the vibrational and magnetic degrees of freedom are not coupled. For $0 < \lambda < 1$ a disordered magnetic structure is elastically softer than the ferromagnetic phase, and for $-1 < \lambda < 0$ the disordered phase is harder than the ferromagnetic phase.

At this point, it is easy to show that the BPM does not satisfy rotation invariance. For instance, given three aligned lattice sites (see Fig. 1) with a nonsymmetric magnetic configuration, a rotation of the crystal gives rise to a net force on the central site, since the bending forces due to the displacement of its neighbors are different. Formally, in the BPM the condition of invariance to rotation on the force constants[18] cannot be satisfied for all magnetic configurations unless the force constants other than stretching vanish. If a given magnetic structure has inversion symmetry, however, in a pure rotation the nonstretching forces cancel, and rotation invariance holds.[16] In a SC lattice this occurs, for example, in ferromagnetic or antiferromagnetic structures in the absence of disorder or in the mean-field approximation, where any

short-range order, apart from what follows statistically from long-range order, is neglected.

Within the framework of cluster expansions it is straightforward to modify the BPM in such a way that it satisfies all the required invariance relations. The natural way is to include additional terms in the spin cluster expansion of the force constants and to impose the invariance conditions on the generalized model.

B. Modified bond proportion model

Our aim is to correct the BPM by introducing the minimum number of changes. Moreover, if possible, we demand that the mean-field solution of the modified and the original bond proportion models be the same for magnetic structures with inversion symmetry. Therefore we have tried to achieve rotation invariance by including terms of the spin cluster expansion that vanish when inversion symmetry is present. To this end, given a pair of atoms, we transform the coordinate system of the corresponding force constant matrix so that the z axis is aligned along the segment joining the two atoms. The diagonal terms, which are the stretching and bending force constants, are not modified. Concerning the off-diagonal terms, the ones which vanish when the magnetic structure has inversion symmetry are written as an expansion of pair clusters. In this expansion we include the pairs of spins containing one of the atoms involved in the force constant, $n, n'(n \neq n')$ and one of its first or second nearest neighbors, n'',

$$\Phi_{nn'}^{ii'} = \sum_{n''} \{(\xi_{nn''})_{nn'}^{ii'} S_n S_{n''} + (\xi_{n'n''})_{nn'}^{ii'} S_{n'} S_{n''}\}. \tag{9}$$

The force constants must be compatible with the symmetries of the magnetic structure. This reduces the number of independent coefficients in Eq. (9). For example, the expansion of the force constant $\Phi_{\mathbf{0},100}^{xy}$ in a simple cubic lattice is reduced to

$$\begin{aligned}\Phi_{\mathbf{0},100}^{xy} = {} & (\xi_{\mathbf{0},010})_{\mathbf{0},100}^{xy} S_{\mathbf{0}}(S_{010} - S_{0\bar{1}0}) + (\xi_{\mathbf{0},011})_{\mathbf{0},100}^{xy} S_{\mathbf{0}}(S_{011} + S_{01\bar{1}} \\ & - S_{0\bar{1}1} - S_{0\bar{1}\bar{1}}) + (\xi_{\mathbf{0},110})_{\mathbf{0},100}^{xy} S_{\mathbf{0}}(S_{110} - S_{1\bar{1}0}) \\ & + (\xi_{\mathbf{0},\bar{1}10})_{\mathbf{0},100}^{xy} S_{\mathbf{0}}(S_{\bar{1}10} - S_{\bar{1}\bar{1}0}) + (\xi_{100,110})_{\mathbf{0},100}^{xy} S_{100}(S_{110} \\ & - S_{1\bar{1}0}) + (\xi_{100,111})_{\mathbf{0},100}^{xy} S_{100}(S_{111} + S_{11\bar{1}} - S_{1\bar{1}1} - S_{1\bar{1}\bar{1}}) \\ & + (\xi_{100,010})_{\mathbf{0},100}^{xy} S_{100}(S_{010} - S_{0\bar{1}0}) \\ & + (\xi_{100,210})_{\mathbf{0},100}^{xy} S_{100}(S_{210} - S_{2\bar{1}0}),\end{aligned} \tag{10}$$

where the indices of the lattice sites, n, n', are expressed in terms of the position coordinates, $x_n y_n z_n$, $x_{n'} y_{n'} z_{n'}$ of the sites.

Next, we impose the condition of invariance of the potential energy to an infinitesimal rotation,[18]

$$\sum_n \Phi_{nn'}^{ii'} r_n^k = \sum_n \Phi_{nn'}^{ki'} r_n^i, \tag{11}$$

where $\mathbf{r}_n$ are the vector positions of the lattice sites. Simultaneously, we require that the on-site force constants matrix, expressed using Eq. (6), be symmetric,

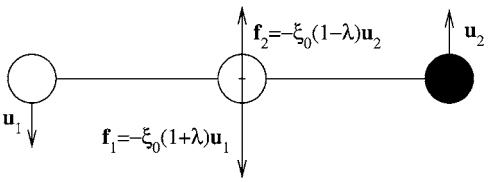

FIG. 1. Three aligned lattice sites with a nonsymmetric magnetic configuration as an example of system where the BPM does not satisfy rotation invariance. Up (down) magnetic spins are shown as white (black) circles. The displacements of atoms due to a rotation $\mathbf{u}_i$ are indicated by arrows, as well as the bending forces acting on the central atom due to these displacements, $\mathbf{f}_i$ (see text for more details).

$$\Phi_{nn}^{ii'} = \Phi_{nn}^{i'i}. \tag{12}$$

These conditions must hold for all magnetic configurations. This sets a system of equations for the coefficients $(\xi_{nn''})_{nn'}^{ii'}$, which imposes that most of them must vanish. The coefficients that remain are related to the parameters of the BPM or are new parameters of the model.

We have solved this problem for a simple cubic crystal structure with interactions up to second nearest neighbors. After cumbersome but straightforward algebra we obtain the following set of force constants:

$$\Phi_{\mathbf{0},100}^{xx} = (\xi_0)_{\mathbf{0},100}^{xx}(1 + \lambda S_{\mathbf{0}} S_{100}),$$

$$\Phi_{\mathbf{0},100}^{yy} = (\xi_0)_{\mathbf{0},100}^{yy}(1 + \lambda S_{\mathbf{0}} S_{100}),$$

$$\begin{aligned}\Phi_{\mathbf{0},100}^{xy} = {} & \lambda S_{\mathbf{0}} \left\{ \frac{1}{4}(\xi_0)_{\mathbf{0},100}^{yy}(S_{010} - S_{0\bar{1}0}) \right. \\ & \left. + \left((\xi_0)_{\mathbf{0},110}^{xx} - (\xi_0)_{\mathbf{0},110}^{xy} - \frac{1}{2}(\xi_0)_{\mathbf{0},110}^{zz} \right)(S_{110} - S_{1\bar{1}0}) \right\},\end{aligned}$$

$$\begin{aligned}\Phi_{\mathbf{0},110}^{xx} = {} & (\xi_0)_{\mathbf{0},110}^{xx}(1 + \lambda S_{\mathbf{0}} S_{110}) - \frac{\lambda}{8}(S_{\mathbf{0}} - S_{110})\{(\xi_0)_{\mathbf{0},100}^{yy}(S_{010} \\ & - S_{100}) + (\xi_0)_{\mathbf{0},110}^{zz}(S_{011} + S_{01\bar{1}} - S_{101} - S_{10\bar{1}})\},\end{aligned}$$

$$\begin{aligned}\Phi_{\mathbf{0},110}^{xy} = {} & (\xi_0)_{\mathbf{0},110}^{xy}(1 + \lambda S_{\mathbf{0}} S_{110}) + \frac{\lambda}{8}(S_{\mathbf{0}} + S_{110})\{(\xi_0)_{\mathbf{0},100}^{yy}(S_{010} \\ & - S_{100}) + (\xi_0)_{\mathbf{0},110}^{zz}(S_{011} + S_{01\bar{1}} - S_{101} - S_{10\bar{1}})\},\end{aligned}$$

$$\Phi_{\mathbf{0},110}^{zz} = (\xi_0)_{\mathbf{0},110}^{zz}(1 + \lambda S_{\mathbf{0}} S_{110}),$$

$$\Phi_{\mathbf{0},110}^{xz} = \frac{\lambda}{4}(\xi_0)_{\mathbf{0},110}^{zz} S_{\mathbf{0}}(S_{101} + S_{011} - S_{10\bar{1}} - S_{01\bar{1}}), \tag{13}$$

where there are no additional free parameters in relation to the BPM.

We remark that if the magnetic structure has inversion symmetry, all the additional terms that we have introduced vanish. Therefore for magnetic structures with this symmetry the mean-field solution of the MBPM is equal to the mean-field solution of the BPM. Notice also that the new terms

depend only on force constants of the BPM other than stretching. Therefore if the original BPM is a stretching force constants model, no correction is made.

III. MEAN-FIELD APPROXIMATION

In this section we solve the BPM in the mean-field approximation for the magnetic degrees of freedom,[1] whereas the vibrational part is treated in the high-temperature limit without any additional approximation. To simultaneously account for both ferromagnetic and antiferromagnetic cases, we separate the system into two sublattices, α and β, and consider only nearest-neighbor interactions in both the magnetic and elastic degrees of freedom. The mean-field approximation is based on the assumption that the spins in the lattice are uncorrelated. Therefore all the properties of the magnetic configurations will depend only on the number of up (+) and down (−) spins at each sublattice, N_α^+, N_α^-, N_β^+, and N_β^-, that is, on the staggered magnetizations, $M_\alpha \equiv 2(N_\alpha^+ - N_\alpha^-)/N$ and $M_\beta \equiv 2(N_\beta^+ - N_\beta^-)/N$ of the sublattices. In particular, the force constants between a pair of nearest-neighbor atoms will be given by

$$\Phi_{nn'}^{ii'}(M_\alpha, M_\beta) = (\xi_0)_{nn'}^{ii'}(1 + \lambda M_\alpha M_\beta). \tag{14}$$

Within this approximation the canonical partition function is

$$\mathcal{Z} = \sum_{M_\alpha} \frac{(N/2)!}{N_\alpha^+ ! N_\alpha^- !} \sum_{M_\beta} \frac{(N/2)!}{N_\beta^+ ! N_\beta^- !} \times \exp\left(\frac{1}{2}\beta J z N M_\alpha M_\beta\right) \mathcal{Z}_v(M_\alpha, M_\beta), \tag{15}$$

where $\beta = 1/k_B T$, z is the nearest-neighbor coordination number and J is the corresponding magnetic exchange constant. The partition function associated with the vibrational degrees of freedom $\mathcal{Z}_v$ is the partition function of a set of $3N$ harmonic oscillators, which in the high-temperature limit is

$$\mathcal{Z}_v(M_\alpha, M_\beta) = \prod_{k=1}^{3N} \frac{1}{\beta \hbar\, \omega_k(M_\alpha, M_\beta)}, \tag{16}$$

where $\hbar$ is the Planck constant and $\omega_k(M_\alpha, M_\beta)$ are the frequencies of the vibrational normal modes.

Since in the thermodynamic limit only the equilibrium value of the magnetization contributes to the partition function, the Helmholtz free energy, $F = -k_B T \ln \mathcal{Z}$, can be written as $F = F_m + F_v$, where

$$F_m = \frac{N k_B T}{2}\left\{\left(\frac{1+M_\alpha}{2}\right)\ln\left(\frac{1+M_\alpha}{2}\right) + \left(\frac{1-M_\alpha}{2}\right)\ln\left(\frac{1-M_\alpha}{2}\right) + \left(\frac{1+M_\beta}{2}\right)\ln\left(\frac{1+M_\beta}{2}\right) + \left(\frac{1-M_\beta}{2}\right)\ln\left(\frac{1-M_\beta}{2}\right)\right\} - \frac{1}{2} J z N M_\alpha M_\beta, \tag{17}$$

and

$$F_v = k_B T \sum_{k=1}^{3N} \ln[\beta \hbar\, \omega_k(M_\alpha, M_\beta)]. \tag{18}$$

The next step is to obtain the dependence of ω_k on the staggered magnetizations. The square of the frequencies of the normal modes are the eigenvalues of the dynamical matrix, which is defined as

$$D_{ii'}(\vec{q}, M_\alpha, M_\beta) \equiv \frac{1}{m} \sum_{nn'} \Phi_{nn'}^{ii'}(M_\alpha, M_\beta) \exp[j\vec{q} \cdot (\vec{R}_{n'} - \vec{R}_n)]. \tag{19}$$

The dynamical matrix can be rewritten as

$$D_{ii'}(\vec{q}, M_\alpha, M_\beta) = (1 + \lambda M_\alpha M_\beta) D_{ii'}(\vec{q}, M_\alpha = 0, M_\beta = 0). \tag{20}$$

Therefore the dependence of its eigenvalues on the staggered magnetizations is

$$\omega^2(\vec{q}, M_\alpha, M_\beta) = (1 + \lambda M_\alpha M_\beta)\omega^2(\vec{q}, M_\alpha = 0, M_\beta = 0), \tag{21}$$

and the contribution to the Helmholtz free energy of the atomic vibrations is

$$F_v = \frac{3}{2} N k_B T \ln(1 + \lambda M_\alpha M_\beta) + k_B T \sum_{k=1}^{3N} \ln[\beta \hbar\, \omega_k(M_\alpha = 0, M_\beta = 0)]. \tag{22}$$

The equilibrium magnetization can be found by minimizing the Helmholtz free energy with respect to the staggered magnetizations M_α, M_β. This leads to the equations

$$\frac{1}{2}\ln\left(\frac{1+M_\alpha}{1-M_\alpha}\right) - \frac{J z M_\beta}{k_B T} + \frac{3\lambda M_\beta}{1 + \lambda M_\alpha M_\beta} = 0,$$

$$\frac{1}{2}\ln\left(\frac{1+M_\beta}{1-M_\beta}\right) - \frac{J z M_\alpha}{k_B T} + \frac{3\lambda M_\alpha}{1 + \lambda M_\alpha M_\beta} = 0, \tag{23}$$

which are solved numerically. From an analysis of the solutions of Eq. (23) together with the evaluation of the corresponding free energy, we obtain the temperatures of first- and second-order phase transitions. The phase diagram of the system is shown in Fig. 2 for ferromagnetic ($J > 0$) and antiferromagnetic ($J < 0$) interactions simultaneously. If the magnetic and vibrational degrees of freedom are not coupled ($\lambda = 0$), we obtain a single second-order phase transition from the low-temperature ferromagnetic (F) or antiferromagnetic (AF) phase to the high-temperature paramagnetic (P) phase. For negative values of $\lambda\, \mathrm{sgn}(J)$ the transition temperature is higher than in the absence of coupling since the low-temperature phase is elastically softer than the paramagnetic phase and thus the vibrational entropy increases its thermodynamic stability. For $\lambda\, \mathrm{sgn}(J) < -1/3$ the vibrational entropy difference between the magnetically ordered and paramagnetic phase cannot be balanced by the corresponding

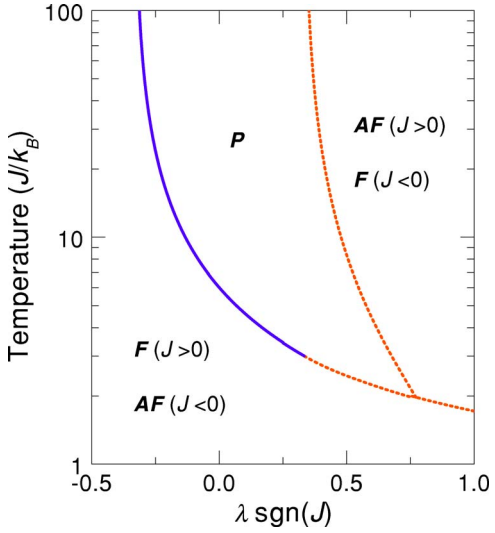

FIG. 2. (Color online) Temperature vs coupling constant, λ sgn(J), phase diagram in the mean-field approximation. Three different magnetic phases are thermodynamically stable: ferromagnetic (F), antiferromagnetic (AF), and paramagnetic (P). The continuous line is a second-order phase transition and discontinuous lines correspond to first-order phase transitions.

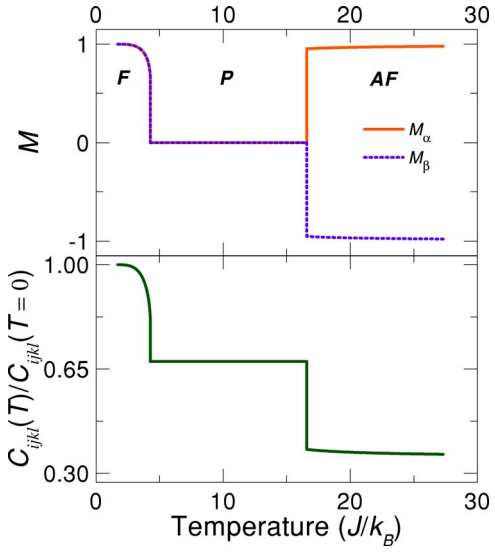

FIG. 3. (Color online) Temperature dependence of the staggered magnetizations and second-order elastic constants for $\lambda=13/27$ and $J=+1$.

magnetic entropy difference and the ordered phase is stable at all temperatures.

For positive values of λ sgn(J) the paramagnetic phase is elastically softer than the ordered low-temperature phase and therefore the transition temperature is lower than in the absence of coupling. For λ sgn(J)$>1/3$, due to the large entropy difference between both phases, the phase transition becomes first order. Moreover, an antiferromagnetic phase for $J>0$ and a ferromagnetic phase for $J<0$ are stabilized at a high enough temperature by vibrational entropy, since this phase is elastically softer than any other magnetic structure. The stability range of the paramagnetic phase decreases with increasing λ sgn(J) and for λ sgn(J)$\geqslant 0.771$ there exists a direct phase transition from the ferromagnetic to the antiferromagnetic phase.

An analytical expression of the transition temperatures for second-order phase transitions is also obtained,

$$T_c^{F-P}(\lambda) = \frac{1}{1+3\lambda}\frac{Jz}{k_B}, \quad J>0,$$

$$T_c^{AF-P}(\lambda) = \frac{-1}{1-3\lambda}\frac{Jz}{k_B}, \quad J<0. \tag{24}$$

The total entropy of the system is obtained from the free energy using the general expression $S=-\partial F/\partial T$. Then, we can estimate the total entropy difference between the magnetic phases. To this end, we characterize the ferromagnetic phase by $M_\alpha=M_\beta\approx\pm 1$, the paramagnetic phase by $M_\alpha=M_\beta\approx 0$, and the antiferromagnetic phase by $M_\alpha=-M_\beta\approx\pm 1$. The estimated entropy differences are

$$\Delta S^{F\to P} \approx Nk_B\ln 2 + \frac{3}{2}Nk_B\ln(1+\lambda) + 3Nk_B\ln\left(\frac{T^P}{T^F}\right),$$

$$\Delta S^{P\to AF} \approx -Nk_B\ln 2 - \frac{3}{2}Nk_B\ln(1-\lambda) + 3Nk_B\ln\left(\frac{T^{AF}}{T^P}\right),$$

$$\Delta S^{F\to AF} \approx -\frac{3}{2}Nk_B\ln\left(\frac{1-\lambda}{1+\lambda}\right) + 3Nk_B\ln\left(\frac{T^{AF}}{T^F}\right), \tag{25}$$

where T^F, T^P, and T^{AF} are the temperatures at which the entropy is evaluated in the ferromagnetic, paramagnetic, and antiferromagnetic phases, respectively.

A convenient measure of the vibrational properties of the system is given by the elastic constants. Defining

$$[ik,jl] \equiv -\frac{1}{2\Omega}\sum_{n'}\Phi^{ik}_{nn'}(r^j_{n'}-r^j_n)(r^l_{n'}-r^l_n), \tag{26}$$

where Ω is the atomic volume, in a Bravais lattice in the absence of stress the second-order elastic constants are related to the force constants through the equation[19]

$$C_{ijkl} = [ik,jl] + [kj,il] - [kl,ij]. \tag{27}$$

Therefore, using Eq. (14), the temperature dependence of the elastic constants in the mean-field approximation can be estimated through the temperature dependence of the staggered magnetizations,

$$C_{ijkl}(T) = (1+\lambda M_\alpha M_\beta)C_{ijkl}(M_\alpha=M_\beta=0)$$
$$= \frac{1+\lambda M_\alpha M_\beta}{1+\lambda\ \mathrm{sgn}(J)}C_{ijkl}(T=0). \tag{28}$$

In Fig. 3 we plot the temperature dependence of both the elastic constants and the staggered magnetizations for $\lambda=13/27$ and $J=+1$. The different stiffness of the magnetic phases due to magnetoelastic coupling is evidenced.

IV. NUMERICAL SIMULATIONS

This section is aimed at computing the thermodynamic properties of the BPM and the MBPM by means of numerical simulation techniques. The differences obtained from both models will be emphasized. In these calculations the range of the force constants is extended up to next-nearest neighbors. In this way, the models are able to fit the three independent elastic constants of a cubic crystal.

The units of energy, mass, length, and temperature are set to be the nearest-neighbors exchange interaction J, the particle mass m, the lattice parameter a, and J/k_B, respectively. All the results are given in these units. The next-nearest neighbors exchange interaction is set to $J_2=2^{-3/2}$, and the coefficients of the cluster expansion are fixed to $(\xi_0)^{xx}_{\mathbf{0},100}=-5\times10^3/(1+\lambda)$, $(\xi_0)^{yy}_{\mathbf{0},100}=-1\times10^3/(1+\lambda)$, $(\xi_0)^{xx}_{\mathbf{0},110}=-2\times10^3/(1+\lambda)$, $(\xi_0)^{xy}_{\mathbf{0},110}=-3\times10^3/(1+\lambda)$, and $(\xi_0)^{zz}_{\mathbf{0},110}=-1\times10^3/(1+\lambda)$. The cluster expansion coefficients are defined in terms of the coupling parameter λ in such a way that the force constants of the low-temperature phase do not depend on λ. With this choice of model parameters the low-temperature magnetic phase is ferromagnetic.

The simulations are performed in a simple cubic structure with $10\times10\times10$ sites with periodic boundary conditions. Since the model Hamiltonian has two well-defined classes of degrees of freedom (magnetic and vibrational) and each has its own characteristic time scale, the dynamics is implemented to each class of degrees of freedom in an independent way. The model dynamics implemented onto the magnetic variables is the spin-flip Metropolis Monte Carlo method, and the time evolution of the vibrational degrees of freedom is simulated by means of Langevin dynamics using the stochastic differential equation,[20]

$$\frac{\partial p_n^i}{\partial t} = -\sum_{n'}\sum_{i'}\Phi_{nn'}^{ii'}u_{n'}^{i'} - \gamma p_n^i + D\eta_n^i(t),$$

$$m\frac{\partial u_n^i}{\partial t} = p_n^i, \tag{29}$$

where $\eta_n^i(t)$ is a Gaussian distributed stochastic variable of zero mean and white in time, $\langle \eta_n^i(t')\eta_n^i(t)\rangle = \delta(t-t')$.

The strength of the dissipative force is set to $\gamma=50$ and the strength of the stochastic force D is related to the strength of the dissipative force γ through the fluctuation-dissipation theorem, $D=\gamma k_B T$. The Langevin equation is integrated using a second-order predictor corrector algorithm[21] with an integration time step $\Delta t=5\times10^{-4}$.

The relation adopted in the simulations between the time scale of the magnetic variables and the time scale of the vibrational degrees of freedom is the following. For each single magnetic spin-flip attempt, five full integration steps of the Langevin equation are performed. The results presented below are obtained as an average over 5×10^5 integration steps after an equilibration period of 15×10^5 integration steps.

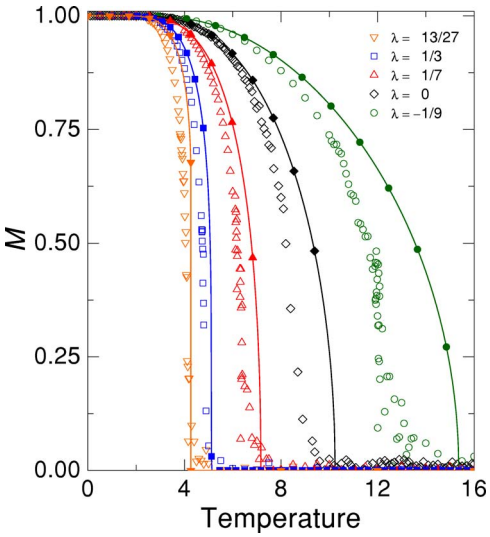

FIG. 4. (Color online) Magnetization vs temperature curves for different values of the coupling constant λ. Open symbols correspond to the results obtained from the numerical simulations and lines with filled symbols are the results of the mean-field approximation.

A. Bond proportion model

In this subsection we present the simulation results corresponding to the BPM which are compared with mean-field results.

1. Magnetization

In Fig. 4 we show the temperature dependence of the magnetization for different values of the coupling constant λ. The results from the numerical simulations (open symbols) are shown together with the results of the mean-field approximation taking into account second-nearest neighbor interactions (lines with filled symbols). It is clear that depending on the sign of the coupling constant λ the transition temperature increases or decreases and the transition is smoother in the former case and sharper in the latter. For large enough values of the coupling constant, the magnetic phase transition becomes first order.

2. Phase diagram

From the temperature dependence of the magnetization, we obtain the magnetic phase diagram of the system (Fig. 5). We restrict ourselves to the ferromagnetic order parameter. Therefore in relation to the phase diagram presented in Fig. 2 we have not analyzed the possibility of stabilizing antiferromagnetic order at high temperature by vibrational entropy. Nevertheless, we expect that the coupling of the second-nearest-neighbor force constants to magnetism will substantially reduce the stability range of this phase in relation to the result presented in Fig. 2.

3. Elastic constants

The isothermal second-order elastic constants are computed using the fluctuation expression[22]

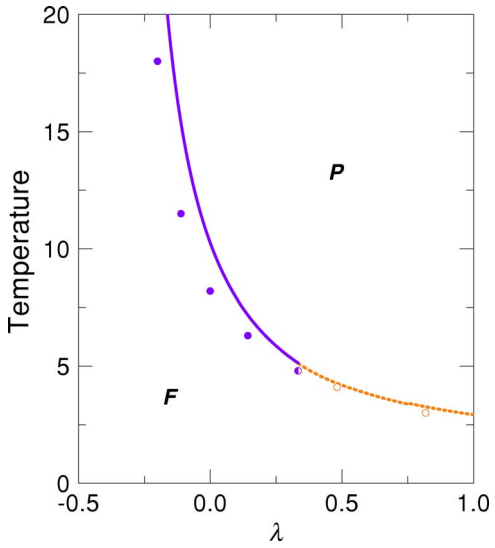

FIG. 5. (Color online) Temperature vs coupling constant λ, magnetic phase diagram showing the ferromagnetic and paramagnetic phases. Circles correspond to the numerical simulations and the line is the result of the mean-field approximation. A second-order phase transition is represented by a continuous line and filled circles, whereas a first-order phase transition is represented by a dashed line and open circles.

$$C_{ijkl}^{T} = \frac{1}{V}\frac{\partial^2 F}{\partial \varepsilon_{ij}\,\partial\,\varepsilon_{kl}} = \frac{1}{V}\left\langle \frac{\partial^2 U}{\partial \varepsilon_{ij}\,\partial\,\varepsilon_{kl}} \right\rangle - \frac{1}{k_B T V}\left\{ \left\langle \frac{\partial U}{\partial \varepsilon_{ij}} \frac{\partial U}{\partial \varepsilon_{kl}} \right\rangle - \left\langle \frac{\partial U}{\partial \varepsilon_{ij}} \right\rangle \left\langle \frac{\partial U}{\partial \varepsilon_{kl}} \right\rangle \right\} + \frac{N k_B T}{V}(\delta_{il}\delta_{jk} + \delta_{ik}\delta_{jl}), \quad (30)$$

where U is the internal energy and ε_{ij} are the components of the elastic strain tensor.

The simulation results of the elastic constant C_{11} are plotted in Fig. 6 together with the results of the mean-field approximation. The temperature behavior of the elastic constants C_{12} and C_{44} is rather similar. It is clear that the presence of magnetic disorder has a strong influence on the elastic constants due to magnetoelastic coupling. Depending on the sign of the coupling constant λ, magnetic disorder increases or decreases the stiffness of the system. Similar behavior has been observed experimentally in order-disorder[12] and magnetic transitions.[13–15]

4. Entropy

The entropy is computed using the thermodynamic relation

$$dS = \frac{C_M}{T} dT, \quad (31)$$

where the heat capacity at constant magnetization is obtained from the fluctuation formula

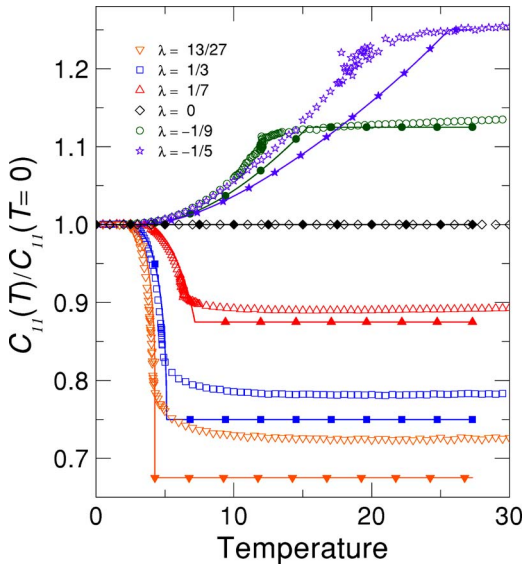

FIG. 6. (Color online) Temperature dependence of the isothermal second-order elastic constant C_{11} for different values of the coupling constant λ. Symbols and lines are the same as in Fig. 4.

$$C_M = \frac{1}{k_B T^2}(\langle U^2\rangle - \langle U\rangle^2), \quad (32)$$

where U is the total energy, including both vibrational and magnetic contributions, $U = U_v + U_m$. If the variance of the total energy is expanded, we obtain

$$C_M = \frac{1}{k_B T^2}(\langle U_v^2\rangle - \langle U_v\rangle^2 + 2\{\langle U_v U_m\rangle - \langle U_v\rangle\langle U_m\rangle\} + \langle U_m^2\rangle - \langle U_m\rangle^2). \quad (33)$$

The first term is the variance of the energy of a set of $3N$ harmonic oscillators, which in the high-temperature limit can be computed analytically,

$$\langle U_v^2\rangle - \langle U_v\rangle^2 = 3N(k_B T)^2. \quad (34)$$

Since the equilibrium energy of an isolated harmonic oscillator does not depend on its frequency, and the time scale of the magnetic degrees of freedom is much slower than the time scale of the atomic vibrations, the vibrational energy of the present model is not coupled to the magnetic degrees of freedom. Thus the second term in Eq. (33) vanishes,

$$\langle U_v U_m\rangle - \langle U_v\rangle\langle U_m\rangle = 0. \quad (35)$$

The effect of coupling between vibrational and magnetic degrees of freedom on the heat capacity is therefore contained in the variance of the magnetic energy. Nevertheless, notice that the effect of magnetoelastic coupling on the entropy is contained in the vibrational entropy term since it depends on the frequencies of the normal modes of oscillation, which, in turn, depend on magnetic order, $S_v = \Sigma_k k_B\{1 + \ln(k_B T/\hbar\omega_k)\}$. Thus we finally obtain

$$dS = \left(\frac{3Nk_B}{T} + \frac{1}{k_B T^3}\{\langle U_m^2\rangle - \langle U_m\rangle^2\}\right) dT. \quad (36)$$

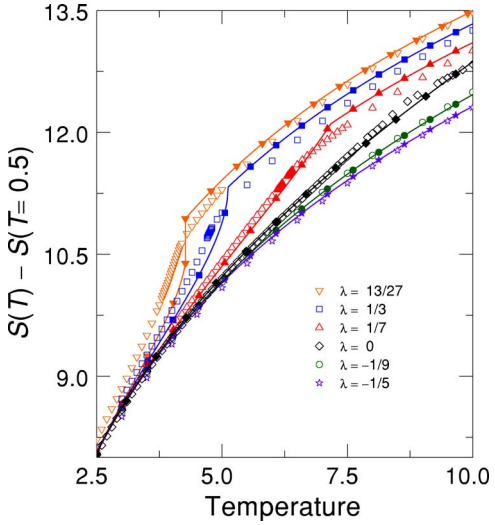

FIG. 7. (Color online) Temperature dependence of the total entropy for different values of the coupling constant λ. Symbols and lines are the same as in Fig. 4.

In Fig. 7 we plot the temperature dependence of the total entropy. The dominant behavior is the logarithmic dependence that arises from the first term of Eq. (36). Close to the magnetic phase transition a substantial increase of the total entropy is observed. This is due to the contribution of the magnetic entropy together with the change in the vibrational entropy due to magnetoelastic coupling. In order to visualize the entropy change at the phase transition, in Fig. 8 we plot the total entropy after subtracting the logarithmic contribution from the vibrational term. It is clear that the total entropy change at the phase transition depends on the coupling parameter λ and the transition is smoother for negative values of λ and sharper for positive values. This is indicative

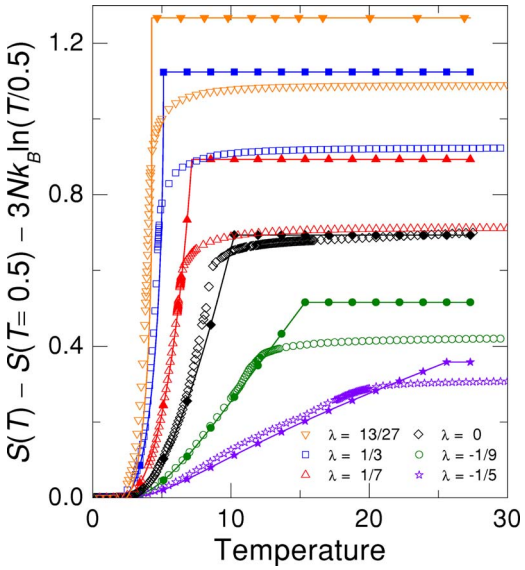

FIG. 8. (Color online) Temperature dependence of the total entropy except for the logarithmic contribution of the vibrational term for different values of the coupling constant λ. Symbols and lines are the same as in Fig. 4.

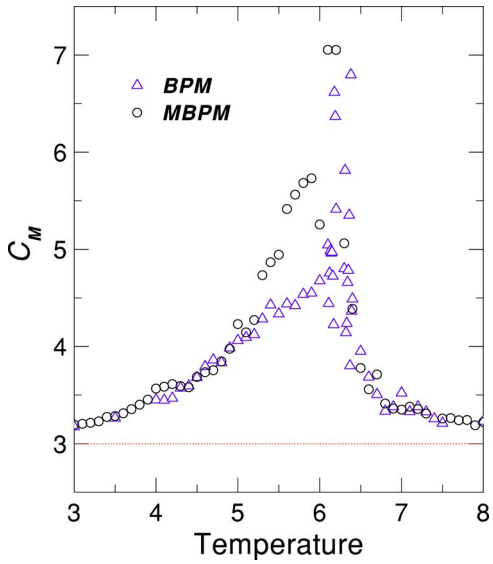

FIG. 9. (Color online) Temperature dependence of the heat capacity of the bond proportion model (triangles) and the modified bond proportion model (circles) obtained from numerical simulations at λ=1/7. The line is the result of a purely vibrational system.

that for negative values of λ the vibrational entropy of the ferromagnetic phase is larger than the vibrational entropy of the paramagnetic phase, and thus the total entropy change is smaller than in the absence of magnetoelastic coupling. On the other hand, for positive values of λ, the vibrational entropy of the paramagnetic phase is larger than the vibrational entropy of the ferromagnetic phase. Note that if the total entropy difference between both phases is large enough, the phase transition becomes first order, whereas if the total entropy difference is small enough, the ferromagnetic phase is stable at all temperatures (see the magnetic phase diagram in Fig. 5).

B. Modified bond proportion model

In this subsection we present the simulation results of the MBPM and analyze the differences obtained in relation to the BPM. All the results correspond to λ=1/7.

In Fig. 9 we show the temperature dependence of the heat capacity at constant magnetization. The difference between both models is significant around the phase transition. Since the models have the same adjustable parameters and lead to the same result when inversion symmetry is present, this discrepancy is indicative that the internal inconsistency of the BPM may be relevant when computing thermodynamic quantities, and that it can give rise to unphysical results. The discrepancy in the heat capacity curves leads to a discrepancy in the entropy difference between the magnetic phases, computed as the integral of the heat capacity over the temperature. This is shown in Fig. 10, where we plot the temperature dependence of the total entropy except for the logarithmic contribution of the vibrational term. Notice that the entropy of the paramagnetic phase given by the MBPM is 30% larger than the entropy given by the BPM.

Finally, in Fig. 11 we show the temperature dependence of the elastic constant C_{11}. The differences between the BPM

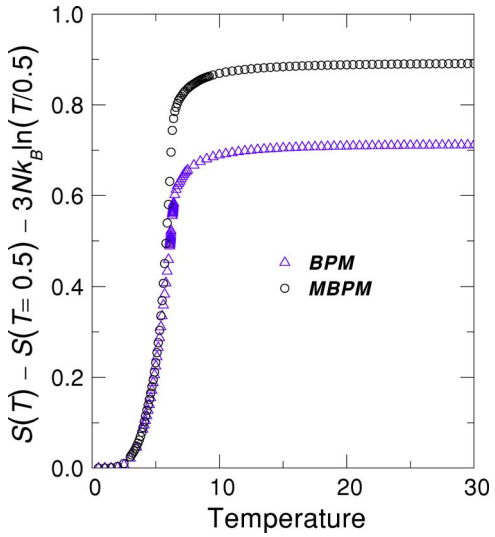

FIG. 10. (Color online) Temperature dependence of the total entropy except for the logarithmic contribution of the vibrational term at $\lambda = 1/7$.

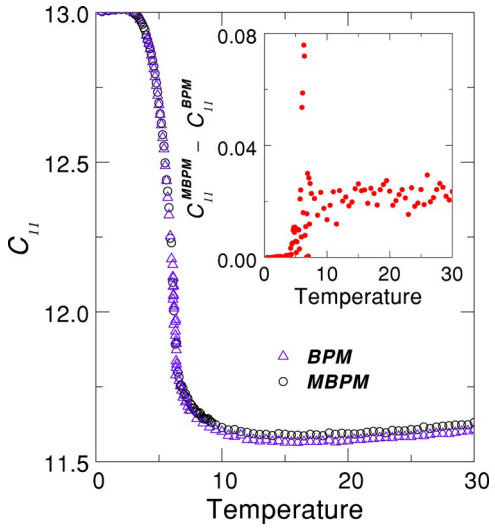

FIG. 11. (Color online) Temperature dependence of the elastic constant C_{11} of the bond proportion model (triangles) and the modified bond proportion model (circles) obtained from numerical simulations at $\lambda = 1/7$. The difference between both results is shown in the inset.

and MBPM are given in the inset. Again, the largest differences are observed around the phase transition, and to a lesser extent, within the paramagnetic phase. As expected, in the ferromagnetic phase both models give rise to the same result.

V. SUMMARY AND CONCLUSIONS

In this paper we have demonstrated that it is possible to develop a harmonic model with coupled configurational and vibrational degrees of freedom that satisfy all the required invariance relations. We have started from the Taylor expansion of the potential energy of a set of N atoms in a lattice. The coefficients of such an expansion are then expanded in clusters of the configurational variables. This method is completely general and turns out to be very powerful.

The bond proportion effect is introduced through the cluster expansion of the force constants. Moreover, atomic relaxations could also be taken into account through the cluster expansion of the linear coefficients of the Taylor expansion. Within this framework we first derive the standard bond proportion model, which does not satisfy the invariance of the potential energy to a rotation of the crystal. We have fixed this problem by including some extra terms in the cluster expansion of the force constants and we have developed a modified bond proportion model. The extra terms choosen are terms that vanish when the magnetic structure has inversion symmetry. In this way, for magnetic structures with this symmetry the mean-field solution of the standard and the modified bond proportion model are equivalent. Both models are solved by means of numerical simulations and it is shown that the bond proportion model gives rise to different results in relation to the modified bond proportion model in the specific heat around the magnetic phase transition, and consequently in the entropy difference between magnetic phases. This is indicative that the bond proportion model may give rise to unphysical results when computing thermodynamic quantities.

Since there is no reason to impose that all the coupling constants of the modified bond proportion model are equal, as assumed in the bond proportion model, the number of independent coefficients of such a model is larger. Therefore the framework of cluster expansions seems to be the ideal candidate to develop configurational independent force constants models that reproduce the vibrational properties of real materials and, at the same time, satisfy all the required invariance relations.

ACKNOWLEDGMENTS

This work was supported by CICyT (Spain) Project No. MAT2004-1291, CIRIT (Catalonia) Project No. 2005SGR00969, and Marie Curie RTN MULTIMAT (Contract No. MRTN-CT-2004-505226).

[1] See, for instance, R. K. Pathria, *Statistical Mechanics*, 2nd ed. (Butterworth-Heinemann, Oxford, 1996), where the thermodynamics of lattice vibration is nicely explained.
[2] G. A. Baker and J. W Essam, Phys. Rev. Lett. **24**, 447 (1970).
[3] E. M. Vandeworp and K. E. Newman Phys. Rev. B **52**, 4086 (1995).
[4] G. A. Baker and J. W. Essam, J. Chem. Phys. **55**, 861 (1971).
[5] B. Dünweg and D. P. Landau, Phys. Rev. B **48**, 14182 (1993).

[6] A. van de Walle and G. Ceder, Rev. Mod. Phys. **74**, 11 (2002).
[7] L. Anthony, J. K. Okamoto, and B. Fultz, Phys. Rev. Lett. **70**, 1128 (1993).
[8] L. Anthony, L. J. Nagel, J. K. Okamoto, and B. Fultz, Phys. Rev. Lett. **73**, 3034 (1994).
[9] B. Fultz, L. Anthony, L. J. Nagel, R. M. Nicklow, and S. Spooner, Phys. Rev. B **52**, 3315 (1995).
[10] J. R. Morris and R. J. Gooding, Phys. Rev. B **43**, 6057 (1991).
[11] There is a simple introduction to the essential physics underlying bond proportion models in H. Bakker and C. Tuijin, J. Phys. C **19**, 5585 (1986).
[12] G. M. McManus, Phys. Rev. **129**, 2004 (1963).
[13] P. de V. du Plessis, S. J. van Tonder, and L. Alberts, J. Phys. C **4**, 1983 (1971).
[14] P. de V. du Plessis and D. L. Tillwick, J. Appl. Phys. **50**, 1835 (1975).
[15] J. F. Collingwood, C. Edwards, S. B. Palmer, J. A. M. Santos, and J. B. Sousa, J. Appl. Phys. **93**, 8349 (2003).
[16] M. H. F. Sluiter, M. Weinert, and Y. Kawazoe, Phys. Rev. B **59**, 4100 (1999).
[17] D. de Fontaine, Solid State Phys. **47**, 33 (1994); in *Density-Functional Methods in Chemistry and Materials Science*, edited by M. Springborg (Wiley, Chichester, 1997), p. 337.
[18] O. Madelung, *Introduction to Solid State Theory* (Springer, Berlin, 1981).
[19] M. Born and K. Huang, *Dynamical Theory of Crystal Lattices* (Clarendon, Oxford, 1956).
[20] R. Kubo, Rep. Prog. Phys. **29**, 255 (1966).
[21] D. C. Rapaport, *The Art of Molecular Dynamics Simulation* (Cambridge University Press, Cambridge, England, 1995).
[22] J. F. Lutsko, J. Appl. Phys. **65**, 2991 (1989).